RSC Advances

PAPER

View Article Online
View Journal | View Issue

Cite this: *RSC Adv.*, 2015, **5**, 35866

Routes towards catalytically active TiO_2 doped porous cellulose†

Alexandra Wittmar,*[ab] Hanna Thierfeld,[ab] Steffen Köcher[a] and Mathias Ulbricht*[ab]

Received 2nd March 2015
Accepted 13th April 2015

DOI: 10.1039/c5ra03707g

www.rsc.org/advances

Cellulose–TiO_2 nanocomposites have been successfully prepared by non-solvent induced phase separation, either from cellulose solutions in ionic liquids or from cellulose acetate solutions in classical organic solvents followed by deacetylation ("regeneration"). Commercially available titania nanoparticles from gas phase synthesis processes have been used and processed as dispersions in the respective polymer solution. The used TiO_2 nanoparticles have been characterized by means of transmission electron microscopy (TEM) and X-ray diffraction (XRD), and their dispersions in ionic liquids and organic solvents have been evaluated by dynamic light scattering (DLS) and advanced rheology. The intermediate polymer solutions used in the phase separation process have been studied by advanced rheology. The resulting nanocomposites have been characterized by means of scanning electron microscopy (SEM) and Fourier transform infrared spectroscopy (FT-IR). Special attention has been given to the complex relationship between the characteristics of the phase separation process and the porous structure of the formed nanocomposites. Two catalytic tests, based on the photocatalytic degradation of model organic dyes under UV irradiation, have been used for the characterization of the TiO_2 doped nanocomposites. The proof-of-concept experiments demonstrated the feasibility of photocatalyst immobilization in porous cellulose *via* phase separation of nanoparticle dispersions in polymer solutions, as indicated by UV-activated dye degradation in aqueous solution.

1. Introduction

Cellulose and its derivatives are among the most important biopolymers. Due to their biocompatibility, biodegradability and renewability they can be used in a large spectrum of applications starting with the already classical ones like the manufacturing of paper,[1] textiles,[2] membranes for water purification and/or biomedical applications[3,4] up to more recent options such as magneto-responsive composites,[5,6] bio-imaging materials[7] or support for catalysts.[8,9]

The processing of pure cellulose is considered difficult because it is insoluble in most common solvents and decomposes before reaching the melting temperature. Usually for the preparation of regenerated cellulose, solutions of cellulose in lithium chloride–dimethylacetamide mixtures, NaOH–thiourea aqueous solutions or aqueous xanthate solutions were used. Its poor solubility is connected with the close packing of the chains *via* intra- and intermolecular hydrogen bonds which are also responsible for the high crystallinity content.[8] More recent studies demonstrate that the addition of triethyloctylammonium chloride salt to acetone enable cellulose dissolution into this solvent by increasing the polarity.[10] Solutions of long chain tetraalkylammonium chloride in organic solvents are also adequate dissolvent media for cellulose.[11] In contrast to cellulose, cellulose derivatives (acetate, nitrate, propionate and butyrate) possess less hydrogen bonding tendency and, consequently, less crystallinity, which allows them to be soluble in common organic solvents like acetone, dimethylformamide (DMF), dimethylsulfoxide (DMSO) *etc.*

It was observed that members of a special class of solvents, room temperature ionic liquids, are able to readily dissolve cellulose in relatively high concentration and without extreme treatments. The term room temperature ionic liquid refers to organic salts which are liquid at temperatures below 100 °C. Most of them have interesting properties like negligible vapor pressure, good thermal stability, large electrochemical window and easy tunability of properties by simple exchanging the anion or cation.[9] Especially the ionic liquids possessing chloride anions, which interact with the hydroxyl groups of cellulose

[a]*Lehrstuhl für Technische Chemie II, Universität Duisburg-Essen, 45141 Essen, Germany. E-mail: alexandra.wittmar@uni-due.de; mathias.ulbricht@uni-due.de; Fax: +49-201-183 3147*

[b]*NETZ – NanoEnergieTechnikZentrum, CENIDE – Center for Nanointegration Duisburg-Essen, 47057 Duisburg, Germany*

† Electronic supplementary information (ESI) available: XRD patterns as well as phase and primary particle size analyses of the TiO_2 P90 nanopowder, TEM micrograph of the TiO_2 P90 nanopowder, TiO_2 P90 particle size distribution in different solvents estimated by DLS, viscosity *vs.* shear rate of cellulose based polymer solutions in different solvents, SEM images of cellulose acetate–TiO_2 composite membranes obtained in different conditions, FT-IR spectra of cellulose acetate and regenerated cellulose membranes, additional results regarding the catalytic activity. See DOI: 10.1039/c5ra03707g

by disrupting hydrogen bonds,[12] are interesting candidates for cellulose processing.

One of the most widely spread method for porous membrane preparation is the phase separation of a polymer solution either induced by temperature change or by immersion into a non-solvent (non-solvent induced phase separation, NIPS).[13] In the NIPS process toward flat-sheet membranes, a solution of the membrane polymer which may contain other additives is cast as thin film on a flat substrate and is then immersed in a precipitation bath which contains the non-solvent which is highly miscible with the polymer solvent. The final pore morphology of the formed membrane depends on the thermodynamic compatibility of the three main components (polymer, solvent, non-solvent), the exchange rate for solvent and non-solvent between film and precipitation bath, the detailed composition of the polymer solution and the coagulation bath, the solvents volatility, and often even some other factors.[14] The preparation of cellulose acetate membranes by NIPS using conventional solvents is long known,[15,16] but the potential of ionic liquids as solvent for porous membrane preparation is still much less and only very recently covered.[17–20]

Introduction of nano-fillers in the cellulosic polymer matrix has been used for modification of the materials properties or to give some additional special functionality. For example, insertion of layered nano-montmorillonite into regenerated cellulose has lead to an improvement of thermal and mechanical stability.[21] Porous cellulose–TiO_2 hybrid materials with bactericidal activity have been successfully prepared.[22] The preparation of cellulose- and cellulose acetate–TiO_2 nanocomposites with photocatalytic properties by complex synthesis procedures has also recently been reported.[23,24] Multifunctional cellulose–Fe_2O_3 nanocomposite fibers have been prepared by *in situ* precipitation of the Fe_2O_3 in the polymer matrix, leading to high mechanical strength, superparamagnetic properties and high dielectric constant.[5] The preparation of magnetite doped cellulose fibers from ionic liquid solutions was reported in 2008.[25]

In this work, cellulose membranes doped with nanoparticles have been prepared by NIPS directly from cellulose solutions in ionic liquids or from cellulose acetate solutions in conventional solvents followed by deacetylation (Fig. 1). For the first time, the successful preparation of cellulose–TiO_2 membranes with anisotropic or sponge-like isotropic pore structure is reported. The influence of the particles presence in the polymer solution on the phase separation and pore formation process has been evaluated. The porous cellulosic films doped with TiO_2 nanoparticles proved to have good catalytic activity in photodegradation of the organic dyes rhodamine B and methylene blue in aqueous solutions.

The focus of the work was set on the effective embedment of commercially available TiO_2 powders into cellulose and cellulose derivatives for the preparation of catalytically active porous nanocomposites. The practical relevance from the materials processing point of view is the straightforward combination of two easily scalable routes, by the integration of nanoparticles from gas phase synthesis technology into formation of porous polymeric membranes by phase separation technology. Among the potential applications of this type of materials are self-cleaning wallpapers which can be used in industrial buildings with high pollutants emissions or easy to clean filters. If the TiO_2 nanoparticles are successfully replaced by, for example, ZnO nanoparticles from gas phase the area of application of these cellulose based nanocomposite materials can be further expanded to the bio-medical sector, *e.g.*, to bactericidal wallpapers with potential application in hospitals.

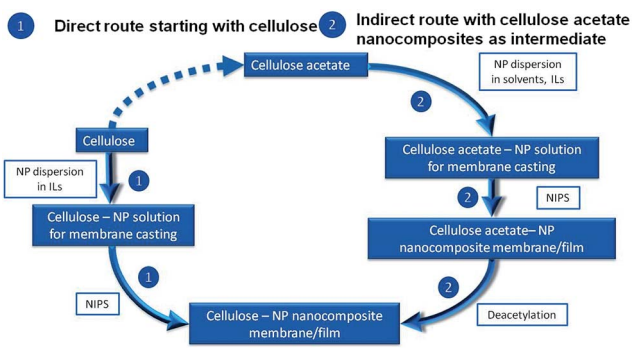

Fig. 1 Alternative routes towards cellulose-nanoparticle (NP) composite films and membranes.

2. Materials and methods

2.1. Materials

Cellulose acetate with a molecular weight $M_n \sim 30\,000$ g mol^{-1} and an acetyl content of 39.8 wt%, as given by the provider, was supplied by Sigma-Aldrich. Microcrystalline cellulose with DP ~ 200 was purchased from VWR International. The ionic liquids 1-butyl-3-methylimidazolium acetate (BmimOAc) and 1-butyl-3-methylimidazolium chloride (BmimCl) were purchased from Sigma-Aldrich and used without further purification. Both ionic liquids as well as cellulose acetate and cellulose are hygroscopic. Because water presence does not hinder the cellulose-based polymers dissolution in ionic liquids, it had been decided to use all precursors "as received" in order to avoid difficult and costly purification processes which would hinder a facile up-scaling of the studied processes. Cellulose acetate solutions were prepared in acetone (p.a.) and dimethylformamide (DMF; p.a.), both supplied by VWR International.

Different metal oxide nanoparticles were purchased as follows: TiO_2 from Sigma Aldrich and Evonik Industries (Aeroxide P90) and Fe_2O_3–TiO_2 mixed oxide from Evonik Industries (Aeroxide TiO_2 PF2).

The dyes used for the catalytic activity tests were methylene blue (hydrate; ≥95%) from Fluka and rhodamine B (96%) from Alfa Aesar.

2.2. Preparation of cellulose based films and membranes

The nanoparticle dispersions in ionic liquids were prepared at the desired concentrations (1, 2.5, 5, 7.5 and 10 wt% with respect to the polymer) by treatment in an ultrasound bath (BANDELIN Sonorex Digitec). Ionic liquid and desired amount of nanopowder were inserted in a snap-cap vial, which was then

suspended in the ultrasound bath and treated 1 h at the power of 80 W. When BmimCl was used, the duration of the sonication was extended to 2 h which allowed the increase of the temperature in the sonication bath to 80 °C and therefore further reduction of the ionic liquids viscosity.

The nanoparticle dispersions in acetone and DMF were prepared at the desired concentrations (2.5, 7.5 or 10 wt% with respect to the polymer) by treatment with a Bandelin Sonoplus Generator GM 2200 ultrasound homogenisator. The solvents and the corresponding amount of powder were introduced in a glass vial and then homogenized for 2 min with amplitude of 30%.

For the preparation of the polymer solutions (with or without nanoparticles) the solvent or NP dispersions were mixed with the desired amount of polymer (8, 10, 12 or 14 wt% with respect to the solvent) and homogenized in a mortar. The mixtures with cellulose were then heated to 70 °C for BmimOAc and 90 °C for BmimCl until complete dissolution of the polymer (*ca.* 1 h). For cellulose acetate solutions in acetone and DMF no heating treatment was necessary, therefore the samples were stirred at room temperature until complete polymer dissolution.

The polymer films were casted on glass substrates with the help of a motorized film applicator (model AB3400 from TQC), using a casting knife with gap width of 300 μm and a speed of 20 mm min^{-1}. When polymer solutions in ionic liquid were casted, the glass plate, casting knife and polymer solution were all preheated to 70–90 °C in order to ensure the fluidity of the polymer solution. The glass supported polymer films were immediately immersed in the coagulation bath consisting of distilled water at RT and were left there for *ca.* 24 h in order to allow completion of phase separation. Subsequently, the membranes were washed with fresh distilled water and dried in air at room temperature or freeze-dried in an Alpha freeze dryer from Christ.

2.3. Characterization methods

The X-Ray Diffraction (XRD) patterns of the TiO_2 P90 powder were obtained using a Bruker D8 Advance powder diffractometer with a Bragg–Brentano geometry (reflexion) and a Si-monocrystal (911 surface) sample holder. The second angles domain of 10 to 90° was chosen to achieve a good statistics of the reflexes. A step size of 0.01°/2Th and a step time of 2 s per measurement were used. The K-beta line was filtered off by a Ni filter foil to ensure an irradiation of the sample by both the K-alpha 1 and the K-alpha 2 (which can be eliminated mathematically later on).

Transmission electron micrographs of the material have been recorded using a Phillips CM 200 FEG equipment.

The rheology of the polymer solutions was studied in rotation mode using an Anton Paar Physica MCR301 rheometer with cone and plate geometry (1°) and Peltier temperature control system. To eliminate any previous shear histories and to allow the samples to establish the equilibrium structures, a steady pre-shear was applied at a shear rate of 1 s^{-1} for 60 s followed by a 120 s rest period before each dynamic rheological measurement. In viscosity *versus* shear rate scans, the shear rates were varied between 0.1 and 1000 s^{-1}. For polymer solutions in ionic liquids, viscosity *versus* temperature studies were performed over a temperature interval from 20 °C to 100 °C, at a constant rotation speed of 9.39 min^{-1} and a heating rate of 10 °C min^{-1}.

The agglomerate size in dispersion, d_{DLS}, was determined by dynamic light scattering (DLS) method using a Particle Metrix Stabisizer heterodyne backscattering equipment at a laser wavelength of 500 nm and a laser power of 5 mW. Each sample was measured three times over a period of 60 s for each run and the result is the average of the three measurements. The corresponding pure ionic liquid was used as reference background for the dispersion in ionic liquid. The DLS data are presented as distribution by number.

Scanning electron micrographs of the porous membranes at different magnifications were taken with a FEI ESEM Quanta 400 FEG instrument. For the cross section measurements the samples were broken in liquid nitrogen. The samples were sputtered with Au/Pd (80/20) at 0.1 mbar and 30 mA for 30 s until a layer of 2–3 nm was obtained.

The results of the deacetylation process were evaluated with help of FT-IR ATR spectroscopy using a Varian 3100 Excalibur series spectrometer with an angle of incidence of 45° and a diamant crystal. The 600–4000 cm^{-1} spectral range was measured with at an average of 32 scans per sample and with a resolution of 4 cm^{-1}.

The catalytic activity of the nanoparticle doped cellulose-based nanocomposites has been evaluated in the photodegradation of organic dyes like methylene blue or rhodamine B in two tests:

1. Membrane pieces of 1 cm^2 were impregnated with aqueous solutions of organic dyes (2×10^{-5} M): each membrane piece was immersed in 30 ml of dye solution and was maintained there in dark conditions for 30 min. The membrane pieces after removal from dye solution were placed in an open crystallizing dish and exposed to the UV radiation (365 nm) in a TLC CN-15 viewing cabinet from Vilber Lourmat GmbH provided with 2 × 15 W lamps and yielding an UV intensity at location of the sample of 1050 μW cm^{-2}. Digital pictures were taken before UV exposure and after specific periods of time (Test 1).

2. In order to assess the photodegradation efficiency in a heterogeneously catalyzed water treatment process, pieces of wet membrane (1 cm^2) or milled dried composite, containing 0.01 g TiO_2, were inserted in 30 ml of aqueous dye solution (5×10^{-5} M). The mixtures were first stirred in dark conditions until the adsorption–desorption equilibrium had been reached, then the samples were exposed for a certain amount of time to UV light (365 nm) under same conditions as in Test 1. Small samples of dye solution were taken periodically by a syringe and the catalyst was filtered off with a 0.2 μm cellulose acetate microfiltration membrane (Sartorius). The variation of dye concentration with irradiation time was followed by UV spectroscopy using an UviLine 9400 Spectrometer from Schott Instruments. The measurements were performed in the 400–800 nm spectral range with a resolution of 1 nm. For comparison purposes, the photo-degradation of 30 ml aqueous dye

solution (5×10^{-5} M) with 0.01 g pure TiO_2 P90 powder was analyzed in analogous manner (Test 2).

3. Results and discussion

3.1. Membranes and films prepared by direct route

The TiO_2 nanoparticles (P90 from Evonik) used for the preparation of nanocomposites and the subsequent catalytic tests have according to the XRD data high anatase content (97%) and only 3% rutile content. The estimated primary particle size for anatase is 10–14 nm and that for rutile 12–17 nm. These particle size distributions calculated from the XRD patterns are in good agreement with the observations in transmission electron micrographs (see ESI, Fig. SI-1 and 2†).

The direct route of film/membrane preparation starting with microcrystalline cellulose and using ionic liquid as solvent has the following advantages: the nanoparticles can be very well dispersed in the ionic liquid (see ESI, Fig. SI-3†) and the formed nanoparticle dispersions have good stability,[26,27] and the whole process has very low VOC emissions. However, some disadvantages have to be taken into account: the polymer can be dissolved into an ionic liquid only up to a certain concentration and the resulting polymer solutions have at room temperature extremely high viscosities, making film casting difficult (see ESI; Fig. SI-4 and SI-5†). As result, the film casting could be performed only at high temperature. The viscosity of a 10 wt% cellulose solution in BmimOAc at 70 °C was ~6 Pa s and that of a 10 wt% cellulose solution in BmimCl at 90 °C was ~7.3 Pa s. Nevertheless, the high viscosity of the polymer solution and the, consequently, slow solvent–nonsolvent exchange contribute to the low porosity of the films formed from ionic liquids solutions. Fig. 2 presents examples of cellulose films, pure or TiO_2 doped, prepared by phase separation from solutions in BmimCl and BmimOAc. Relevant characteristics of these films are their strong shrinkage during drying process and their brittleness. The addition of TiO_2 nanoparticles slightly reduced the shrinkage but also slightly increased the brittleness.

As a consequence of a very slow exchange between water and ionic liquid, the NIPS process takes considerably longer than for polymer precipitation from organic solvent solutions. The porosity of the films prepared from ionic liquid solutions can be increased by increasing the temperature at which the phase separation takes place which increases the rate of the solvent–nonsolvent exchange, by reduction of the polymer content in the casting solution, but also by freeze drying the wet membrane or by a combination of above mentioned procedures (see ESI; Fig. SI-6†).

Fig. 3 presents exemplary pore morphologies of cellulose–TiO_2 films prepared by NIPS from ionic liquids solutions. One may very clearly observe that there is a clear correlation between the porosity of the resulting material and the viscosity of the corresponding polymer solution: the higher the viscosity of the casting solution, the more compact is the corresponding film. Additionally, one may observe that for highly viscous polymer solutions the quality of dispersion of the nanoparticles in the matrix became worse. This may be explained by the following phenomena: at the beginning of the cellulose dissolution, the system consists in a mixture of nanoparticle dispersion in ionic liquid and cellulose dispersion in the same ionic liquid. Progressively the cellulose swells and the oxidic nanoparticles

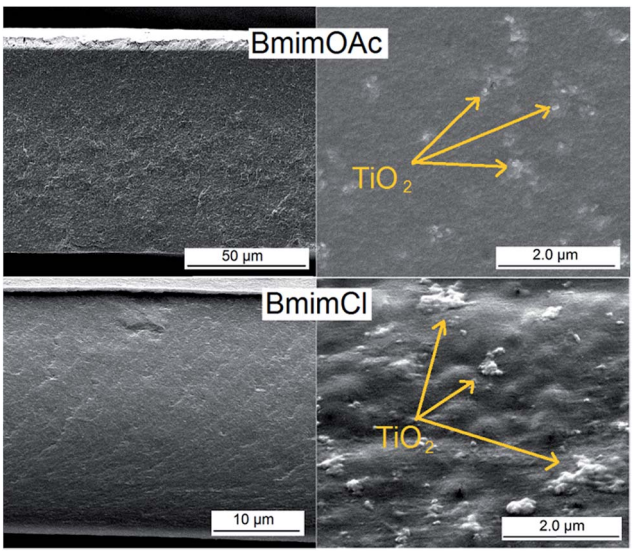

Fig. 3 Scanning electron microscopy images (left: cross-section; right: top view) of cellulose–TiO_2 P90 (ratio: 20 : 1) nanocomposite films from 10 wt% cellulose solutions in ionic liquid. (note the different magnification for the material prepared from BmimCl).

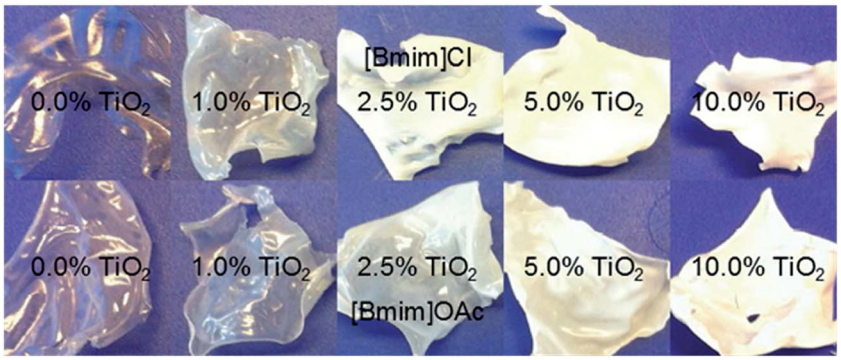

Fig. 2 Cellulose–TiO_2 (Aldrich) nanocomposite films obtained from ionic liquid solutions.

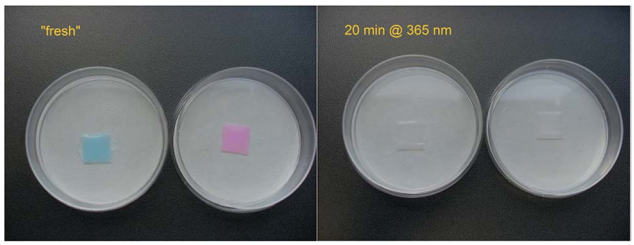

Fig. 4 Photocatalytic degradation of methylene blue and rhodamine B on cellulose–TiO_2 P90 (ratio: 10 : 1) nanocomposite films from ionic liquid solutions.

tend to be trapped between swollen cellulose particles. In the case of casting solutions with lower viscosity there still is a chance to improve the particle dispersibility in the polymer solution post polymer dissolution by mechanical stirring. This is not the case of the highly viscous casting solutions.

The photocatalytic activity of cellulose–TiO_2 (10 : 1) was demonstrated on polymer films impregnated with dye solutions as described in "Test 1" (in chapter 2.3). By simple irradiation with a UV source, the adsorbed dye was completely decomposed in short exposure time: *ca.* 10 min for methylene blue and *ca.* 20 min for rhodamine B (Fig. 4). This type of experiment was performed only to demonstrate the existence of photocatalytic activity and had no quantitative aspect.

However, this type of materials proved to be less effective in the catalytic "Test 2" (described in chapter 2.3). The lack of activity in this test may be explained by the fact that due to the low porosity only a small amount of dye is able to come in direct contact with the active oxide species and the removal of products from the surface is also poor. One may expect an increase of the activity in Test 2 by increasing the porosity of the nanocomposite material.

Diluted TiO_2 doped polymer solutions in ionic liquids may also be used for the surface modification of filters and membranes or in direct membrane preparation by electrospinning.

3.2. Films and membranes prepared by indirect route

The indirect route of preparation implies in a first step the preparation of a cellulose acetate solution which will be used for membrane casting. Due to the possibility to solubilize cellulose acetate in a wide range of solvents, casting solutions of this polymer with lower viscosity may be readily obtained (see ESI; Fig. SI-5†), facilitating the casting process. Additionally, the use of a much wider range of solvents also allows detailed control of the phase separation process, enabling the formation of pores with desired morphology (Fig. 5). However, nanoparticles dispersibility in these solvents is considerably poorer when compared with the ionic liquids (see ESI; Fig. SI-3†).

The cellulose acetate membranes obtained from phase separation can in a second step relatively easily be transformed in cellulose membranes by simple deacetylation ("regeneration"). The structure of the resulting cellulose membranes only partially retains the pore structure of the cellulose acetate precursor. The thickness and the pore morphology of the cellulose film differs from the corresponding cellulose acetate intermediate, partially due to a collapse of the pores which takes place during the deacetylation process and partially due to loss of the acetyl groups (Fig. 6). However some of the features of the cellulose acetate membrane may still be observed in the final material. Another route which should be explored in the future works is the precipitation of the cellulose acetate film directly in a 0.1 N NaOH solution in water/ethanol which may directly lead

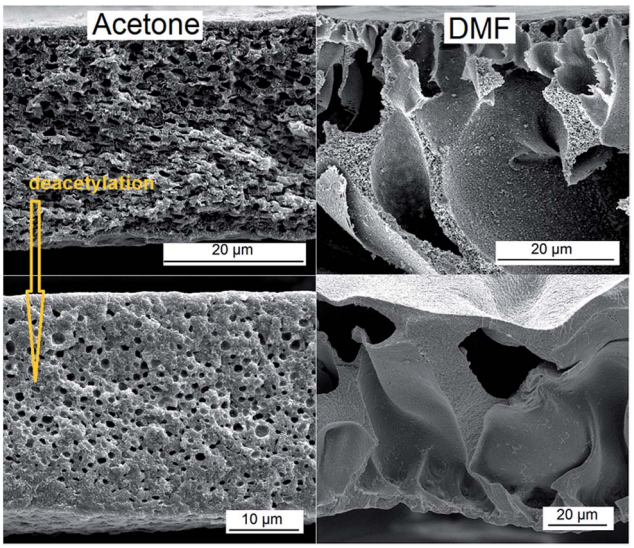

Fig. 6 Scanning electron microscopy images (cross-section) of cellulose structures obtained by deacetylation of the corresponding cellulose acetate precursors prepared from two different solvents.

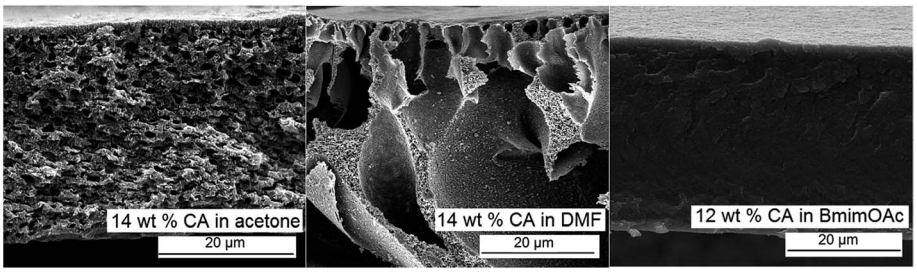

Fig. 5 Scanning electron microscopy images (cross-section) of cellulose acetate membranes prepared by NIPS from solutions in different solvents.

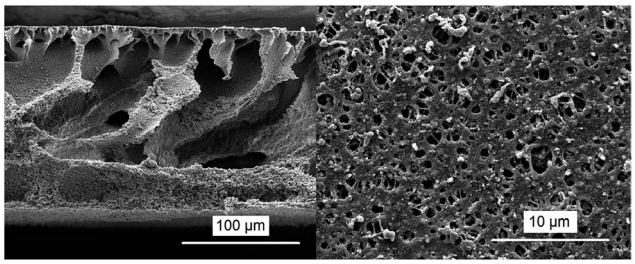

Fig. 7 Scanning electron microscopy images (left: cross-section; right: top view) of cellulose acetate–TiO_2 P90 (ratio: 10 : 1) membrane prepared by phase separation from a DMF solution.

to the formation of a regenerated cellulose membrane after the complete removal of the acetyl groups during the phase separation cum regeneration.

When nanoparticles are dispersed in the cellulose acetate solvent, metal oxide doped casting solutions may be obtained, and further on, cellulose acetate nanocomposite membranes with different structures will be formed after the subsequent NIPS step. The greater majority of the organic solvents which can be used for cellulose acetate dissolution, in pure form, are poor dispersants for the not functionalized nanoparticles. Therefore an additional optimization step represented by nanoparticles functionalization and/or dispersion stabilization should be involved for optimal results. In the present work, this optimization step was not addressed, because the intention had been to elucidate the possible advantages of this two-step method for the pore formation process. Fig. 7 shows an example of a catalytically active TiO_2-doped cellulose acetate membrane which has been prepared from a polymer solution in DMF. The addition of 10 wt% of TiO_2 nanoparticles did not seem to have a significant influence on the pore formation mechanism. Examples of cellulose acetate-based and corresponding cellulose-based membranes with different fractions of TiO_2 are presented in ESI (Fig. SI-7 and 8†). The success of the deacetylation process was demonstrated by FT-IR ATR spectroscopy (see ESI; Fig. SI-9†).

The catalytic activities of the cellulose acetate nanocomposites and of the corresponding deacetylated materials have been demonstrated by photodegradation of organic dyes (10^{-5} M in water). The methylene blue was completely degraded after 30 min exposure to UV radiation @ 365 nm, while the rhodamine B was completely degraded in *ca.* 1 h in similar conditions (see ESI; Fig. SI-10†). In order to quantify the catalytic activity of the TiO_2 immobilized in the polymer matrix, a series of experiments ("Test 2"; *cf.* Methods) was performed. The rate constants were calculated assuming that the concentration of dye in solution is proportional to the intensity at the absorption maximum in the UV-vis spectrum. It was observed that under the described conditions, rhodamine B did not decompose in the absence of the catalyst (Fig. 8a). A wet cellulose acetate–TiO_2 (ratio: 10 : 1) membrane and milled dried composite with similar composition were catalytically active, but with rate constant an order of magnitude lower than the not immobilized titania (Fig. 8a and Table 1).

This considerably lower photodegradation efficiency of the membrane-based catalysts was expected, on one hand because of the clearly lower specific surface of the active material due to partial agglomeration and on the other hand due to the partial embedment in the cellulose matrix (no direct contact to the dye solution). Mass transfer may be improved by convective flow of the solution through the porous membrane.

After the deacetylation process one can observe a further reduction of the photocatalytic activity which may be explained by the partial collapse of the pores (Fig. 8b and Table 1). A

Table 1 Rate constant k for the photocatalytic degradation of rhodamine B, from experiments with different catalysts with same TiO_2 content

Material	k [min^{-1}]
TiO_2 P90	0.03155 ± 0.0068
Cellulose acetate–TiO_2 P90 (ratio: 10 : 1) wet membrane	0.00375 ± 0.0004
Cellulose acetate–TiO_2 P90 (ratio: 10 : 1) milled dried composite	0.00265 ± 0.0004
Regenerated cellulose–TiO_2 P90 milled dried composite	0.00088 ± 0.0001

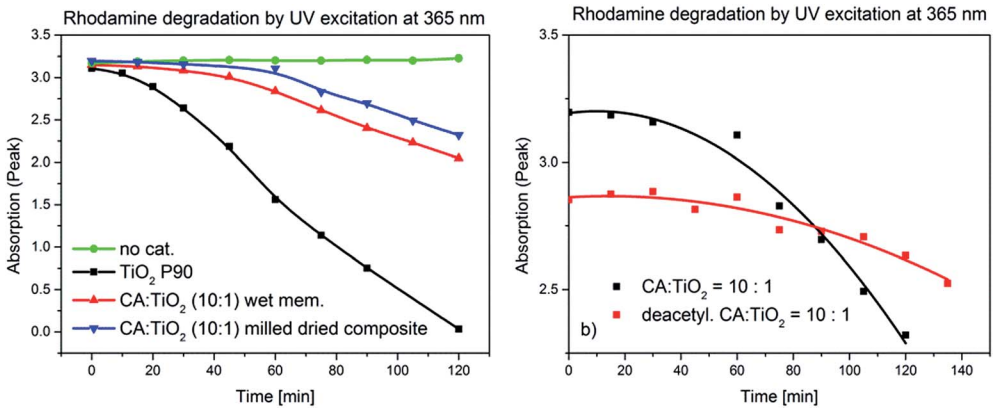

Fig. 8 (a) Rhodamine B degradation with different photocatalytically active materials; (b) rhodamine B degradation cellulose acetate–TiO_2 P90 (ratio: 10 : 1) milled dried composite and corresponding regenerated cellulose–TiO_2 P90 (ratio: 10 : 1) milled dried composite.

possible explanation for a lower starting point of the decomposition curve in the case of the deacetylated polymer may be more dye adsorption on the deacetylated polymer surface.

A direct comparison between the catalytic activities of cellulose–TiO_2 materials prepared from polymer solutions in ionic liquids with a material of same composition prepared by the two step process was not possible. However one may postulate that the tested dyes adsorb less on the denser cellulose materials prepared by the direct route, leading to a drastic decrease of the degradation rate.

The performed two catalytic tests offer only preliminary results. Further studies, including analysis of total organic carbon (TOC), will in depth study the mineralization of the dyes during the photocatalytic processes. Another issue that should be addressed in the following studies is evaluation of the actual content of TiO_2 within the composite as well as the leaching of the active TiO_2 nanoparticles from the polymer matrix during the phase separation and during use. Additionally, the lifetime and reusability of such photocatalytically active nanocomposites will be evaluated.

4. Conclusions

In the present work, new alternative routes for the preparation of nanoparticle-doped porous cellulose-based materials with potential applications in the fields of catalysis and health care have been discussed. Two important aspects have been addressed: the development of environmentally friendlier processes for cellulose processing by replacing of the conventional VOC solvents with "greener" ionic liquids and the replacement of the *in situ* nanoparticle generation from expensive alkoxide precursors with the use of economically efficient nanoparticles prepared by highly scalable synthesis reactions in gas phase. Both preparation routes presented in Fig. 1 proved to be suited for the preparation of nanoparticle-doped cellulose-based nanocomposites, allowing relative good nanoparticle distribution within the porous polymer matrix. The dispersibility of the nanoparticles in the solvents used for polymer solubilisation and in the polymer solution itself may be further improved by pre-functionalization. Even though the ionic liquids are excellent solvents for cellulose, being able to dissolve concentrations higher that 20 wt%, they have the disadvantage of yielding highly viscous polymer solutions which hinders the casting process. Additionally, deriving from the high viscosity, the phase separation process takes place very slowly resulting in materials with very low porosity. Pore control and design for these systems are difficult but may be improved by increasing the temperature at which the phase separation is performed or by addition of a co-solvent with lower viscosity. Supplementary, diluted TiO_2 doped polymer solutions in ionic liquids may find potential use in the filters surface modification or for membrane formation by electrospinning. The alternative two-step route offers an advanced control of the pore formation by the choice of the adequate solvent but the not functionalized nanoparticles have a poor dispersibility in most of the suited organic solvents. All cellulose and cellulose acetate intermediates exhibit photocatalytic activity against organic dyes when doped with TiO_2. The porous structure and the distribution of the nanoparticles within the polymer matrix proved to have a crucial influence on the catalytic efficiency of the resulting hybrid nanocomposites. The newly generated nanocomposites are not intended as replacements for the TiO_2 already established in catalytic processes; they have potential to be used as cellulosic materials with an extra function: here catalytic activity under UV irradiation. The presented results suggested that some of these materials may find applications like, for example, self cleaning wallpapers or easy to clean filters.

Acknowledgements

We gratefully acknowledge the collaboration with Mr Smail Boukercha (SEM characterization), Dr Oleg Prymak (XRD characterization) and Dr Wolfgang Meyer-Zaika (TEM characterization) at the University of Duisburg-Essen.

References

1 J. Langley and D. Holroyd, *US Pat.*, 4 913 775, 1990.
2 R. C. Law, *Macromol. Symp.*, 2004, **208**, 255.
3 N. Hoenich, *BioResources*, 2006, **1**, 270.
4 G. M. Geise, H. S. Lee, D. J. Miller, B. D. Freeman, J. E. Mcgrath and D. R. Paul, *J. Polym. Sci., Part B: Polym. Phys.*, 2010, **48**, 1685.
5 S. Liu, L. Zhang, J. Zhou and R. Wu, *J. Phys. Chem. C*, 2008, **112**, 4538.
6 J. Shen, Z. Song, X. Qian and Y. Ni, *Ind. Eng. Chem. Res.*, 2011, **50**, 661.
7 S. Dong and M. Roman, *J. Am. Chem. Soc.*, 2007, **129**, 13810.
8 L. Zhang, D. Ruan and S. Gao, *J. Polym. Sci., Part B: Polym. Phys.*, 2002, **40**, 1521.
9 J. P. Hallet and T. Welton, *Chem. Rev.*, 2011, **111**, 3508.
10 M. Kostag, T. Liebert and T. Heinze, *Macromol. Rapid Commun.*, 2014, **35**, 1419.
11 M. Kostag, T. Liebert, O. A. El Seoud and T. Heinze, *Macromol. Rapid Commun.*, 2013, **34**, 1580.
12 M. Mazza, D. A. Catana, C. Vaca-Garcia and C. Cecutti, *Cellulose*, 2009, **16**, 207.
13 P. Van der Witte, P. J. Dijkstra, J. W. A. van der Berg and J. Feijen, *J. Membr. Sci.*, 1996, **117**, 1.
14 G. R. Guillen, Y. Pan, M. Li and E. M. V. Hoek, *Ind. Eng. Chem. Res.*, 2011, **50**, 3798.
15 M. T. So, F. R. Eirich, H. Strathmann and R. W. Baker, *J. Polym. Sci., Polym. Lett. Ed.*, 1973, **11**, 201.
16 M. A. Frommer and R. M. Messalem, *Ind. Eng. Chem. Prod. Res. Dev.*, 1973, **12**, 328.
17 X. L. Li, P. L. Zhu, B. K. Zhu and Y. Y. Xu, *Sep. Purif. Technol.*, 2011, **83**, 66.
18 D. Y. Xing, N. Peng and T. S. Chung, *Ind. Eng. Chem. Res.*, 2010, **49**, 8761.
19 D. Y. Xing, N. Peng and T. S. Chung, *J. Membr. Sci.*, 2011, **380**, 87.
20 B. Ma, A. Qion, X. Li and C. He, *Ind. Eng. Chem. Res.*, 2013, **52**, 9417.

21 S. Mahmoudian, M. U. Wahit, A. F. Ismail and A. A. Yussuf, *Carbohydr. Polym.*, 2012, **88**, 1251.
22 S. M. Li, Y. Y. Dong, M. G. Ma, L. H. Fu, R. C. Sun and F. Xu, *Carbohydr. Polym.*, 2013, **96**, 15.
23 X. Jin, J. Xu, X. Wang, Z. Xie, Z. Liu, B. Liang, D. Chen and G. Shen, *RCS Adv.*, 2014, **4**, 12640.
24 Y. Luo, J. Xu and J. Huang, *CrystEngComm*, 2014, **16**, 464.
25 N. Sun, R. P. Swatloski, M. L. Maxim, M. Rahman, A. G. Harland, A. Haque, S. K. Spear, D. T. Daly and R. D. Rogers, *J. Mater. Chem.*, 2008, **18**, 283.
26 A. Wittmar, M. Gajda, D. Gautam, U. Dörfler, M. Winterer and M. Ulbricht, *J. Nanopart. Res.*, 2013, **15**, 1463.
27 A. Wittmar, D. Gautam, C. Schilling, U. Dörfler, W. Meyer-Zaika, M. Winterer and M. Ulbricht, *J. Nanopart. Res.*, 2014, **16**, 3241.